The $^3F_3$ Nucleon-Nucleon Partial-Wave Scattering Amplitude as a Resonance Plus a Background.

R. BHANDARI

Department of Physics, Virginia Polytechnic Institute and State University Blacksburg, Va. 24061, U.S.A.

(ricevuto l'11 Marzo 1982)

Summary. – Recent comprehensive partial-wave analyses of the world nucleon-nucleon elastic scattering data show structure in the $^3F_3$ partial-wave scattering amplitude in the $(2.15 \div 2.30)$ GeV centre-of-mass energy region. Interpreting this structure as the result of a resonant behaviour, we present a complete set of resonance parameters by representing the amplitude as a smoothly varying background plus a resonance.

The idea of dibaryon resonances has always been controversial [1]. Recently, the observation of structure in $\Delta\sigma_L$ (the difference between the proton-proton total cross-sections for parallel and antiparallel longitudinal spin states) at intermediate energies ($\sim(2.15 \div 2.35)$ GeV) renewed further interest in their possible existence [2]. In fact, HIDAKA *et al.* [3] interpreted the afore-mentioned structure as being due to a resonant behaviour in the $^3F_3$ nucleon-nucleon partial-wave amplitude. Furthermore, in roughly the same energy region, recent independent, comprehensive analyses [4,5] of the world nucleon-nucleon scattering data show sharp energy variation in the $^3F_3$ phases. In order to understand the origin of this observed structure, several authors [6,7] subsequently performed an energy-dependent coupled-channel T-matrix analysis of the $^3F_3$ partial-wave amplitude. An accurate fit to the recent, precise phase shifts of Arndt

---

(1) F. J. DYSON and N. H. XUONG: *Phys. Rev. Lett.*, **13**, 815 (1964); R. A. ARNDT: *Phys. Rev.*, **165**, 1834 (1968); L. M. LIBBY and E. PREDAZZI: *Lett. Nuovo Cimento*, **18**, 881 (1969); H. SUZUKI: *Prog. Theor. Phys.*, **54**, 143 (1975); D. D. BRAYSHAW: *Phys. Rev. Lett.*, **37**, 1329 (1976).

(2) See A. YOKOSAWA: Argonne National Laboratory preprint No. ANL-HEP-PR-80-16 which includes a review of the experimental situation.

(3) H. HIDAKA, A. BERETVAS, K. NIELD, H. SPINKA, D. UNDERWOOD, Y. WATANABE and A. YOKOSAWA: *Phys. Lett. B*, **70**, 479 (1977).

(4) N. HOSHIZAKI: *Prog. Theor. Phys.*, **60**, 1976 (1978).

(5) R. A. ARNDT, L. D. ROPER, B. J. VERWEST, R. CLARK, R. A. BRYAN and P. SIGNELL: *Nucleon-nucleon partial-wave analyses from the Virginia Polytechnic Institute and State University dial-in system*, to be published.

(6) B. J. EDWARDS: *Phys. Rev. D*, **23**, 1978 (1981); W. M. KLOET and J. A. TJON: *Phys. Lett. B*, **106**, 24 (1981); B. J. VERWEST: Texas A and M University preprint (1981).

(7) R. BHANDARI, R. A. ARNDT, L. D. ROPER and B. J. VERWEST: *Phys. Rev. Lett.*, **46**, 1111 (1981).

et al. [5] by authors of [7] revealed an influential pole coupled mainly to the $\mathcal{N}\Delta$ channel. In this letter, we report a complete set of the traditional resonance parameters by fitting a Breit-Wigner form in conjunction with a smoothly varying background to the ${}^3F_3$ phases of Arndt *et al.* [5].

By writing the elastic S-matrix element S as a product of the resonant part S_R and the background S_B, the elastic partial-wave amplitude T is

$$T = (S_B S_R - 1)/(2i) = S_B T_R + T_B , \tag{1}$$

where

$$T_R = (S_R - 1)/(2i) , \tag{2a}$$

$$T_B = (S_B - 1)/(2i) . \tag{2b}$$

In terms of the parameter η and the phase shift δ,

$$S = S_B S_R = \eta \exp[2i\delta] . \tag{2c}$$

The Breit-Wigner resonance amplitude T_R is

$$T_R = \frac{\gamma_e^2 \Phi_e}{E_R - E - i\gamma_e^2 \Phi_e - i \sum_j k_j^2 \Phi_j} , \tag{3}$$

where the index j runs over the inelastic channels. The elastic and the inelastic phase space factors, Φ_e and Φ_j, are functions of the centre-of-mass energy E. The coupling parameters, γ_e and γ_j, and the parameter E_R are freely varied in the fit. The form for the background S-matrix element S_B used in the analysis is

$$S_B = \frac{1 + \sum_{j=1}^{2} a_j E^j + i \sum_{j=1}^{3} b_j E^{j-1} \Phi_e - \sum_k \{c_k^2 + d_k^2 (E - E_k)\} \Phi_e \Phi_k}{1 + \sum_{j=1}^{2} a_j E^j - i \sum_{j=1}^{3} b_j E^{j-1} \Phi_e + \sum_k \{c_k^2 + d_k^2 (E - E_k)\} \Phi_e \Phi_k} , \tag{4}$$

where E_k is the threshold energy for the inelastic channel k. Parameters a_j, b_j, c_k and d_k are free. Below E_k, Φ_k is completely imaginary. Thus S_B is unitary. That is, $|S_B|$ is equal to 1 for $E_e < E < E_1$, where E_e and E_1 are the threshold energies for the elastic and the first inelastic channels, respectively. Furthermore, it is less than 1 for $E > E_1$. In a similar fashion, one observes that the S-matrix element S_R obtained from eqs. (2*a*) and (3) satisfies the same unitarity constraint.

Above a laboratory kinetic energy T_L of ~ 290 MeV, inelasticity in the $\mathcal{N}\mathcal{N}$ amplitudes sets in due to pion production originating mainly in the $\mathcal{N}\Delta$ channel [8]. The phase shifts of ARNDT *et al.* [5] presently exist up to 800 MeV, and have very small errors. We supplemented these with two data points of Hoshizaki [9] which lie beyond

---

[8] S. MANDELSTAM: *Proc. R. Soc. London Ser. A*, **244**, 491 (1958).
[9] N. HOSHIZAKI: private communication to R. A. ARNDT [5].

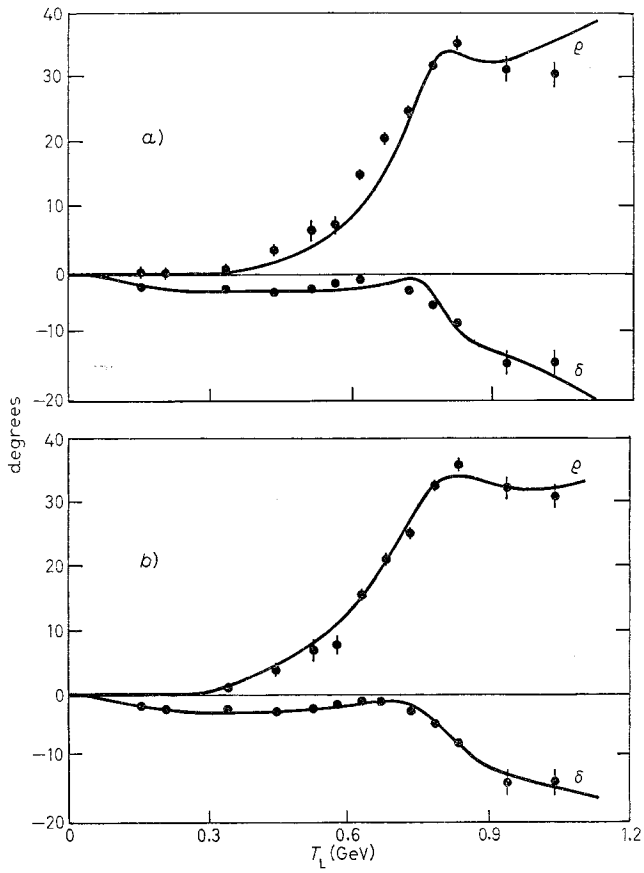

Fig. 1. – Fit to the $^3F_3$ nucleon-nucleon partial-wave phases, using *a)* $\mathcal{N}\Delta$ as the only inelastic channel, *b)* $\mathcal{N}\Delta$ and πD (pion-deuteron) as the inelastic channels. δ is the conventional phase-shift, while ϱ is related to the parameter η by $\eta = \cos^2\varrho$. T_L is the laboratory kinetic energy of the incident nucleon.

$T_L = 800$ MeV. Starting with $\mathcal{N}\Delta$ as the only inelastic channel, we obtained a reasonable fit shown in fig. (1*a*)). The phase ϱ is related to the parameter η by $\eta = \cos^2\varrho$. The fit improves significantly with the inclusion of the pion-deuteron (πD) channel, and is shown in fig. (1*b*)). The phase-space factors used for the three channels are

$$(5a) \qquad \Phi_0 = \Phi_{\mathcal{N}\mathcal{N}} = \{(E - E_{\mathcal{N}\mathcal{N}})/(E - r_0)\}^{\frac{7}{2}},$$

$$(5b) \qquad \Phi_1 = \Phi_{\pi D} = \{(E - E_{\pi D})/(E - r_1)\}^{\frac{5}{2}},$$

$$(5c) \qquad \Phi_2 = \Phi_{\mathcal{N}\Delta} = \frac{1}{(E - r_2)^{\frac{3}{2}}} \int_{M_T = M_{\mathcal{N}} + M_\pi}^{\infty} \frac{\{(E - (M_{\mathcal{N}} + M))\}^{\frac{3}{2}} (M - M_T)^{\frac{3}{2}} \, dM}{(M + \alpha)^3 [(M - M_0)^2 + \Gamma^2/4]}.$$

They have the appropriate threshold behaviour corresponding to relative orbital-angular-momentum values of 3, 2, 1 for the $\mathcal{N}\mathcal{N}$, πD and $\mathcal{N}\Delta$ channels, respectively.

$E_{\mathcal{N}\mathcal{N}}$ and $E_{\pi\mathrm{D}}$ are the threshold energies for the $\mathcal{N}\mathcal{N}$ and πD channels. The phase-space factor in the case of the $\mathcal{N}\Delta$ channel is a quasi-two-body one describing the production of the Δ isobar (in conjunction with $\mathcal{N}$) and its subsequent decay into $\mathcal{N}$ and π with a relative orbital angular momentum of 1. Because of its variable mass, an integration is performed. The Breit-Wigner factor in the denominator corresponds to a complex mass $M - i\Gamma/2$ for Δ, which we take to be $(1.21 \div i.05)$ GeV. $M_{\mathcal{N}}$, M_{π} are nucleon, pion masses, respectively. The parameters r_e, r_1 and r_2 which give rise to left-hand cuts are phenomenological in nature, having values less than $E_{\mathcal{N}\mathcal{N}}$. They essentially control the behaviour of the phase-space factors, ensuring that they do not rise to extraordinarily large values away from their respective thresholds. In our fits, r_e, r_1 and r_2 were ~ 1.8, ~ 1.8, and ~ 10.5 GeV, respectively. Figure 2 shows the right-hand unitarity cut structure along with the $\mathcal{N}\Delta$ branch cuts which the elastic amplitude T acquires from the above phase-space factors. The $\mathcal{N}\Delta$ cuts lie on unphysical sheets associated with the three-body $\mathcal{N}\mathcal{N}\pi$ cut [10], with the first $\mathcal{N}\Delta$ cut in fig. 2 reached immediately by following arrow 2 from the top of the unitarity cuts. Cuts at the complex-conjugate position of the $\mathcal{N}\Delta$ branch point also occur on these unphysical sheets, but are not shown in fig. 2. For completeness, we may also remark that branch points at $E = M_{\mathcal{N}} - \alpha$ due to the form factor $1/(M+\alpha)^3$ [10] in eq. (5*c*) are also present on these unphysical sheets. But, since the parameter α is assigned a value greater than $-M_{\mathcal{N}}$ (typical value being ~ -0.93) in order that these cuts lie to the left of the elastic threshold, we have not shown them in fig. 2. The above form factor, it may be noted, also ensures the convergence of the integral in eq. (5*c*). Analytic expression for this integral exists [10].

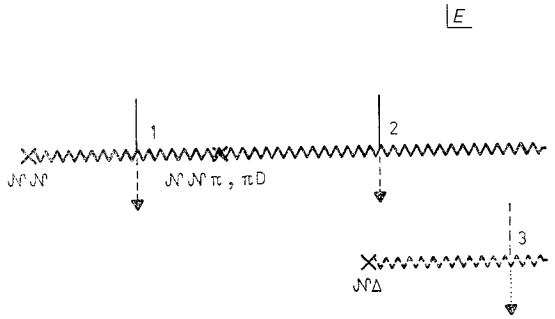

Fig. 2. – The right-hand cut structure of the elastic ${}^3F_3$ amplitude T in the complex-E plane. Because of the close proximity of the $\mathcal{N}\mathcal{N}\pi$ and πD channels, a single branch point is shown for them. Arrows indicate the different unphysical sheets that can be reached.

The dip in the phase shift and the bump in the ϱ phase (near ~ 0.7 GeV) in fig. 1*a*) and *b*) result from the presence of a resonance. Its parameters are calculated from the following definitions:

i) The mass M_{R} of the resonance corresponds to the real energy at which the real part of the denominator D_{R} in eq. (3) vanishes.

ii) The full-width $\Gamma_{\mathrm{R}} = -2 \operatorname{Im} D_{\mathrm{R}}(M_{\mathrm{R}})$.

---

[10] R. BHANDARI: *Phys. Rev. D* (in press).

iii) The ratio of partial-widths to the full width Γ_R are

$$e_{\mathcal{N}\mathcal{N}} = \Gamma_{\mathcal{N}\mathcal{N}}/\Gamma_R\,, \qquad \Gamma_{\mathcal{N}\mathcal{N}} = 2\gamma_e^2\,\Phi_{\mathcal{N}\mathcal{N}}(M_R)/\Gamma_R\,,$$
$$e_{\pi D} = \Gamma_{\pi D}/\Gamma_R\,, \qquad \Gamma_{\pi D} = 2\gamma_1^2\,\Phi_{\pi D}(M_R)/\Gamma_R\,,$$
$$e_{\mathcal{N}\Delta} = \Gamma_{\mathcal{N}\Delta}/\Gamma_R\,, \qquad \Gamma_{\mathcal{N}\Delta} = 2\gamma_2^2\,\mathrm{Re}\,(\Phi_{\mathcal{N}\Delta}(M_R))/\Gamma_R\,.$$

iv) The observed pole lies on the unphysical sheet reached from the top of the right-hand unitarity cuts, and corresponds to $D(E_p) = 0$, where $E_p = M_p - i\Gamma_p/2$ is the pole position. When $\Gamma_p/2$ exceeds $\Gamma/2 = 0.05$ in fig. 2, it lies on the sheet indicated by arrow 3. Near the pole, the amplitude T may be expressed as

$$T = \frac{R}{E_p - E} + \ldots\,, \tag{6}$$

where R is the residue of the pole. From eqs. (1) and (3), one finds that

$$R = -\frac{S_B(E_p)\gamma_e^2\,\Phi_{\mathcal{N}\mathcal{N}}(E_p)}{(\partial D_R(E)/\partial E)|_{E=E_p}}\,. \tag{7}$$

TABLE I. – *Resonance parameters for the observed $^3F_3$ dinucleon resonance.* See text for definition of parameters.

real part of the pole position, M_p	(2.218 ÷ 2.200) GeV
imaginary part of the pole position, Γ_p	(0.045 ÷ 0.06) GeV
magnitude of the residue R	(0.005 ÷ 0.006) GeV
phase of the residue R	(−5 ÷ 4)°
mass of the resonance, M_R	(2.251 ÷ 2.266) GeV
half-width of the resonance, $\Gamma_R/2$	(0.07 ÷ 0.10) GeV
elasticity $e_{\mathcal{N}\mathcal{N}}$	(0.11 ÷ 0.13)
parameter $e_{\pi D}$	(0.2 ÷ 0.3)
parameter $e_{\mathcal{N}\Delta}$	(0.6 ÷ 0.7)

Table I gives the range of values of the resonant parameters determined from the set of best fits, one of which is shown in fig. 1*b*). The fits being tightly constrained by the small errors on the data points determine the resonance parameters, especially M_p, R, M_R and e_1, fairly well. The pole position, especially the real part, is much more stable than the mass M_R and the half-width $\Gamma_R/2$ of the resonance. Also one notes from the table that the amount of πD channel in the resonance, although small with respect to the $\mathcal{N}\Delta$ channel, is nevertheless significant. Figure 3 displays the Argand plot of the amplitude along with its real and imaginary parts calculated as a function of the centre-of-mass energy E from the fit shown in fig. 1*b*).

In summary, by separating the background from the $^3F_3$ $\mathcal{N}\mathcal{N}$ partial-wave amplitude, we have determined the parameters of the resonance responsible for the structure in the (2.15 ÷ 2.30) GeV centre-of-mass energy region. Indications for its existence have existed before ([2-4,6]). This particular analysis is a single-channel analysis, utilizing

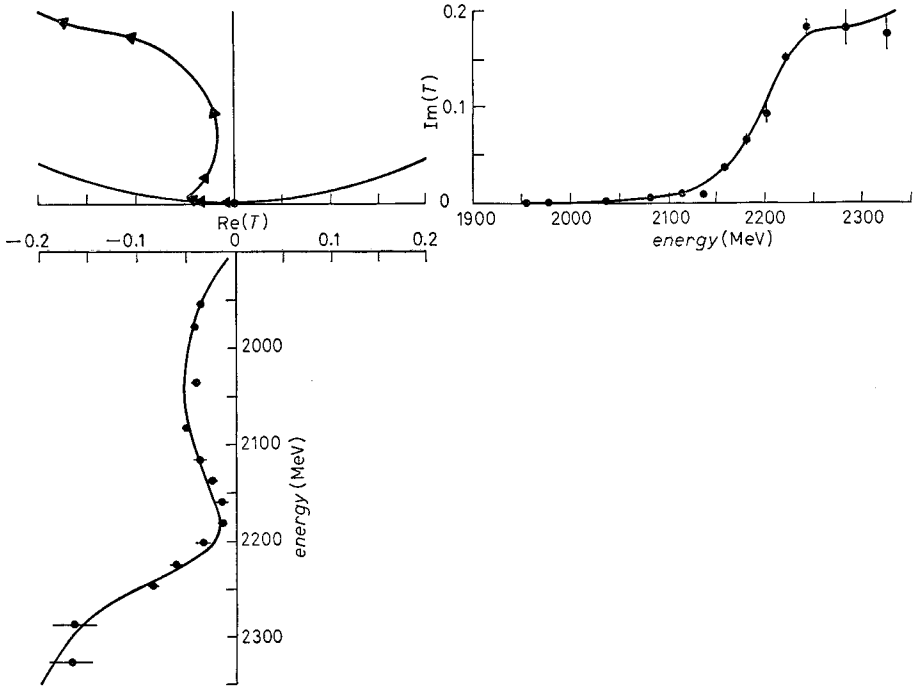

Fig. 3. – Argand plot of the ${}^3F_3$ $\mathcal{N}\mathcal{N}$ amplitude along with its real and imaginary parts separately shown as a function of the centre-of-mass energy E. Arrows on the Argand plot are at 50 MeV intervals with the topmost corresponding to $E = 2300$ MeV. Any two arrows which are very close are shown as a single arrow.

a parametrization which has the appropriate unitarity property and the right-hand cut structure. An essential feature of our fit is the significant coupling of the πD channel to the resonance. Previous analyses (coupled-channel) ([6,7]) either ignore πD channel completely or do not find it coupled appreciably to the πD resonance.

* * *

The author thanks Profs. R. A. ARNDT and L. D. ROPER for permitting him to use computer facilities and some of their computer programs. This work was supported by the U.S. Department of Energy.